

1 *Published in:*

2 **Tree Physiology**

3 <https://doi.org/10.1093/treephys/tpv126>

4 **Effect of soil temperature on root resistance:**
5 **implications for different trees under**
6 **Mediterranean conditions**

7 OMAR GARCÍA-TEJERA^{1,3}, ÁLVARO LÓPEZ-BERNAL¹, FRANCISCO J.
8 VILLALOBOS^{1,2}, FRANCISCO ORGAZ¹ and LUCA TESTI¹

9 ¹Instituto de Agricultura Sostenible (IAS), Consejo Superior de
10 Investigaciones Científicas (CSIC), Alameda del Obispo, s/n, 14004, Córdoba,
11 Spain

12 ²Departamento de Agronomía, Edificio Celestino Mutis, Campus de
13 Rabanales, Universidad de Córdoba, 14014, Córdoba, Spain

14 ³Corresponding author (ogarcia@ias.csic.es)

15 **Abstract**

16 The effect of temperature on radial root hydraulic specific resistance (R_p) is a known
17 phenomenon; however, the impact of R_p variations expected from soil temperature changes
18 over the tree root system is unknown. The present article analyses the relationship of R_p
19 with temperature in olive 'Picual' and a hybrid rootstock, GF677, at five different
20 temperatures, showing that a variation of 3- and 4.5-folds exists for olive 'Picual' and
21 GF677 in the range from 10 to 20 °C. The functions obtained were scaled up to show the
22 theoretical changes of total radial root system resistance in a common tree orchard in a
23 Mediterranean climate at a daily and seasonal scale, using recorded soil temperature values:
24 a difference between summer and winter of 3.5-fold for olive 'Picual' and 9-fold for GF677
25 was observed. Nevertheless, R_p changes are not only related to temperature, as cavitation or
26 circadian rhythms in aquaporin expression may also play a role. The results obtained from
27 an experiment with the two cultivars submitted to constant pressure and temperature during
28 several hours exhibited a variation in R_p , but this was of lower magnitude than that
29 observed due to temperature changes. Finally, a comparison of R_p at 25 °C between GF677
30 and GN15 (another rootstock obtained from the same parental as GF677) showed
31 significant differences. According to our results, diurnal and seasonal changes in R_p due to
32 temperature variations are of significant importance, and it would therefore be advisable to
33 assess them explicitly into soil–plant–atmosphere continuum models.

34 **Keywords:** compensated heat pulse, stem water content, TDR, *Olea europaea*, water
35 relations.

36 **Introduction**

37 Models of the soil–plant–atmosphere continuum (SPAC) are powerful tools to improve our
38 insight into plant water relation traits. The movement of water through the plant can be
39 compared to an electric circuit composed of a catena of resistances in series or parallel and
40 with the differences in water potential as the driving force. This simplification of the
41 hydraulic system was first proposed by Van den Honert (1948) and is widely used in SPAC
42 models (Williams et al. 2001, Couvreur et al. 2012). According to that simple approach,
43 plant transpiration (E_p) can be written as:

44
$$E_p = \frac{\varphi_s - \varphi_l}{R_{soil} + R_{plant}} \quad (1)$$

45 where R_{soil} is the soil resistance, i.e., the resistance of water movement from the soil to the
46 root xylem, R_{plant} is the plant resistance that includes the resistance of the xylem of roots,
47 stem and branches, and Ψ_s and Ψ_l are soil and leaf water potential, respectively. If one
48 focuses on the soil part of the equation, R_{soil} can be divided into two resistances in series:
49 the hydraulic specific resistance of the soil (R_s) for the movement of water from the bulk
50 soil to the root surface and the hydraulic specific resistance of the root in the radial
51 direction (R_p), that is, the resistance from the root surface to xylem vessels. The equation
52 now would be:

53
$$E_p = \frac{\varphi_s - \varphi_l}{R_s + R_p + R_{plant}} \quad (2)$$

54 According to Eq. (2), variations in R_p due to shifts in the root environment would affect E_p ,
55 but how important is R_p in relation to the other terms of Eq. (2)?

56 Experiments on trees have revealed that shoot and root resistances are approximately equal
57 (Tyree and Zimmermann 2002). When the soil is wet, R_s is much lower than R_p (Campbell
58 1985); hence, R_{soil} would be approximately equal to R_p . If R_{plant} and R_{soil} are nearly the
59 same, in theory, the changes in R_p would have a significant impact on E_p under the above-
60 mentioned conditions.

61 Variations in E_p due to shifts in root temperature have been described for different species
62 (Kramer 1940, Running and Reid 1980, Lee et al. 2004). Still in the nineteenth century,
63 Sachs (1870) observed that well-watered tobacco plants growing in conditions of low
64 evaporative demand wilted when soil temperature was decreased to 3 °C and they
65 recovered when the soil was warmed to 12 °C. Kramer (1940) and Ameglio et al. (1990)
66 also observed a reduction in E_p of ~80% in tomato and sunflower, when the root system
67 was cooled down to 5 and 2.7 °C, respectively, when compared with its values at 20 °C.
68 The changes on transpiration are not unique to herbaceous species; trees like *Populus*
69 *tremuloides* Michx., *Quercus rubra* L or *Olea europea* L also show a reduction in
70 transpiration when the temperature of the root system is decreased below a certain value
71 (Pavel and Fereres 1998, Wan et al. 2001, Apostol et al. 2007).

72 Different hypotheses have been proposed to explain the effect of low root temperature on
73 the reduction in E_p . The increase of water viscosity as temperature decreases has been
74 suggested as the main factor for reducing water flow from the soil to the plant (Yamamoto
75 1995, Hertel and Steudle 1997). Other authors hypothesized that the phenomenon
76 originates from changes in membrane permeability due to modifications of its fluidity, or
77 reductions in the activity of membrane aquaporins (Running and Reid 1980, Ameglio et al.
78 1990, Wan et al. 2001, Lee et al. 2004). Leaving aside the mechanisms involved, it seems

79 to be clear that changes in root temperature modify radial root hydraulic specific
80 conductance, or its inverse, R_p .

81 Environmental factors are not the exclusive causal agents for changes in R_p , but the plant
82 itself presents endogenous rhythms related to its ability to uptake water. Henzler et al.
83 (1999) found a 24-h cycle of one order of magnitude in *Lotus japonicus* L when the root
84 system was submitted to a constant pressure. The authors attributed those changes to a
85 circadian rhythm in the aquaporin expression of the root system. Besides, Tyree and
86 Zimmermann (2002) discovered a 24-h cyclic pattern of the same order of magnitude in
87 root water conductivity in plants whose roots were held at a constant pressure for 3 days. In
88 their experiment, carried out with tobacco plants using a wild type and a mutant with the
89 NtAQp1 aquaporin protein suppressed, both the mutant and the wild type showed exactly
90 the same pattern, suggesting that no aquaporin was involved in the circadian cycle or at
91 least that type of aquaporin.

92 Although variations in R_p among cultivars, soil conditions and even according to
93 endogenous rhythms have been widely described in the literature, the value of R_p used to
94 compute root water uptake in SPAC models is usually a fixed parameter (Doussan et al.
95 1998, Williams et al. 2001). However, Mellander et al. (2006) demonstrated that a
96 significant improvement in the prediction of transpiration can be achieved by taking into
97 account the delayed temperature of the soil during the spring season using the empirical
98 reduction function of E_p proposed originally by Axelsson and Ågren (1976).

99 As far as we know, the effect of temperature on R_p is unknown for olive and fruit tree
100 rootstocks. For that reason, the aims of the present article are to (i) study the variations of

101 R_p with temperature for olive (*Olea europaea* L.) ‘Picual’ and *Prunus amygdalus* L ×
102 *Prunus persica* L ‘GF677’, the former being one of the more extensively grown olive oil
103 cultivars in Spain, while the latter is a widely used hybrid rootstock for peach, plum and
104 almond trees; (ii) analyse the effect of the above-mentioned variations of R_p with
105 temperature in a tree orchard, using recorded soil temperature data and scaling-up from a
106 single root to an entire root system using reported values of root length density (L_v); (iii)
107 study the presence or absence of other sources of variation in R_p other than temperature,
108 such as a circadian rhythm; and finally, (iv) compare R_p values of the above-mentioned
109 ‘GF677’ rootstock with *P. amygdalus* × *P. persica* ‘GN15’, another rootstock with the
110 same parental species. At the end of the paper, an appendix including a list of abbreviations
111 is provided.

112 **Material and Methods**

113 *Plant material*

114 The experiment was performed with rooted cuttings of olive ‘Picual’ and of two hybrid
115 rootstocks of *P. amygdalus* × *P. persica*, ‘GF677’ and ‘GN15’, obtained from commercial
116 nurseries in Spain. Hereinafter, we will refer to each of the two hybrid rootstocks studied as
117 GF677 and GN15, while the term ‘olive’ alone is to be intended as the cultivar ‘Picual’.
118 The 1-year-old cuttings were transported from the nursery to the experimental greenhouse
119 in August (both *Prunus*) and September 2014 (olive). Once in the experimental greenhouse,
120 cuttings were planted in pots filled with peat moss, where they were irrigated every day in
121 order to avoid water stress. The cuttings stayed no longer than 1 month in the greenhouse
122 before starting the measurements in the growth chamber. Table 1 presents the mean values

123 and the standard deviation (SD) for height and root area of the cuttings used in the
124 experiments. Cuttings were transferred from the greenhouse to the growth chamber 3 days
125 before the start of the experiments to allow for adaptation.

126

127 Table 1. Shoot height and total root area for the cultivars used in this study.

	Shoot height (m)	Root area (m ²)
Olive	0.15 ± 0.05 (n = 25)	0.012 ± 0.0040 (n = 25)
GF677	0.30 ± 0.07 (n = 25)	0.022 ± 0.010 (n = 25)
GN15	0.28 ± 0.05 (n = 25)	0.0074 ± 0.0029 (n = 5)

128

129 All the measurements were done in one growth chamber with controlled temperature,
130 monitored continuously using a data logger (MicroLite, Fourier Systems, USA) and a fixed
131 14-h photoperiod with fluorescent lights at 360 $\mu\text{mol m}^{-2} \text{s}^{-1}$. All the necessary material to
132 perform the experiment was left inside the growth chamber in order to keep everything at
133 the same temperature as the plant material.

134 *Experiment 1: determination of the radial root hydraulic specific resistance at different*
135 *temperatures*

136 The radial root resistance at five temperatures, namely 10, 15, 20, 25 and 30 °C, were
137 measured for GF677 and olive cuttings using four plants for each temperature. At each air
138 temperature, the four cuttings were transferred from the greenhouse to the growth chamber.
139 Values of R_p at each temperature were measured using a pressure chamber (Soil Moisture

140 Equipment Corp., Santa Barbara, CA, USA) adapted to measure flow from a root system.
141 To this end, a pot filled with water was set into the pressure vessel of the chamber in order
142 to supply water to the root system. Plants were extracted from their pots and immersed in
143 water to remove part of the substrate taking extreme care to not disturb the root system.
144 Then the upper part of the cuttings was cut 5 cm above the plant collar; the remaining shoot
145 stub was covered with paraffin from the collar to 1 cm below the cut in order to avoid any
146 radial flux of water into it. The detached root system was then fixed to the specimen holder
147 of the pressure chamber using an appropriate rubber seal, in such a way that after the
148 chamber closure, the root system was completely immersed in water. All the measurements
149 were performed inside the growth chamber at the corresponding temperature (± 0.5 °C) to
150 avoid any thermal shock to the root system.

151 Four different pressures were applied at each temperature: 0.4, 0.6, 0.8 and 1.2 MPa. The
152 xylem sap flowing through the root system at each pressure was collected during periods of
153 15 min using cotton-filled sample tubes previously weighted in a four decimal precision
154 balance (model AV104, Mettler Toledo, Greifensee, Switzerland). The mass of the sample
155 tube plus the xylem sap after 15 min was obtained from the same precision balance. The
156 flux was then calculated by dividing the difference of dry and wet mass of the tube by the
157 time interval. The process was repeated until the difference in flux between measurements
158 was $<0.5\%$. Obtaining a steady value for the flux usually took from 30 to 50 min.

159 Once the fluxes at the given temperature and at the five pressures were obtained, the root
160 system was carefully washed with water to remove all the remaining substrate and was then
161 scanned using a commercial scanner (HP Scanjet G3110). Values of root length average

162 diameter and total root surface were obtained using the WinRhizo software (Regent
163 Instruments Inc., Quebec City, QC, Canada).

164 The inverse of the slope of the linear fit of flux versus pressure was taken as the total root
165 radial resistance of the plant at the corresponding temperature. Specific resistance of each
166 plant was then obtained by dividing the total root radial resistance by its total root surface,
167 assuming a maximum diameter of 1.4 mm for an absorbing root. For each temperature, R_p
168 was averaged for the four plants.

169 The function of R_p versus temperature in olive and GF677 cuttings was fitted using the
170 software TableCurve 2D (SYSTAT Software Inc., San Jose, CA, USA) and fitted using a
171 power function as proposed by Ameglio et al. (1990).

172 *Experiment 2: rootstocks comparisons*

173 Values of R_p for the two rootstocks were obtained following the same method as in
174 Experiment 1. During the experiment, the temperature was kept at 25 °C. Five cuttings of
175 both GF677 and GN15 were used. An analysis of variance (ANOVA) was applied to
176 compare the R_p values of the two rootstocks.

177 *Experiment 3: test of stability of radial root hydraulic specific resistance in steady* 178 *conditions*

179 The validity of the relationships from Experiments 1 and 2 is subjected to the absence of
180 other sources of variation in R_p during the measurements, such as circadian rhythms related
181 to daily variations in the expressions of aquaporins (Henzler et al. 1999), cavitation in the
182 xylem vessels (Espino and Schenk 2011) or any other causes of instability. The presence of

183 such behaviours would cause errors in the measurements of Experiments 1 and 2, and a
184 consequent incorrect function of temperature. To determine the presence and magnitude of
185 endogenous rhythms or any other variation of R_p not related to temperature changes, a
186 stability test in cuttings of olive and GF677 was performed. The temperature of the growth
187 chamber was fixed at 30 °C, and a constant pressure of 0.4 MPa was maintained in the
188 pressure chamber. Values of R_p during 5 h (from 9:00 to 14:00 UTC) were obtained for
189 both species, following the same procedure described for Experiment 1. The experiments of
190 stability for the two species were started at the same relative circadian time as Experiment
191 1, i.e., 8 h after turning the chamber lights on.

192 *Soil temperature and scaling-up of radial root hydraulic specific resistance*

193 To scale the variation of the radial resistance with the soil temperature up to the whole root
194 system, an elementary model was used. The scaling-up for the entire root system can be
195 done by invoking the electric circuit similarity proposed by Van den Honert (1948). For our
196 purposes, the specific resistance of the electric circuit is R_p , which varies with the
197 temperature. Specific resistance represents the resistance per square metre of root surface.
198 To use L_v as a scaling factor, a conversion from square metre of root surface to square
199 metre of soil must be done using an average root radius (a). Root length density is then
200 distributed through different layers in the soil and RR (the resistance per square metre of
201 soil of the whole root system) is computed as:

$$202 \quad RR = \frac{1}{\sum 2\pi a d_i L_{vi} / R_p(T)_i} \quad (3)$$

203 where d is the thickness of soil layer i .

204 Soil temperature profile data (see Figure S1) were recorded over 3 years, from June 2002 to
205 September 2004, in an experimental olive orchard at the ‘Alameda del Obispo’
206 experimental farm located in Córdoba, Spain (37°52’N, 4°49’W). The climate is
207 Mediterranean, with mild and rainy winters and very hot and dry summers; in the period of
208 data collection, the maximum and minimum air temperatures were 47.1 and –1.1 °C,
209 registered on 1 August 2003 and 20 January 2004, respectively. The soil is a
210 ‘TypicXerofluvent’ of sandy-loam texture. Soil thermocouples (type K) were installed at
211 five depths: 5, 10, 20, 40 and 80 cm; the thermocouple outputs were read every minute, and
212 10-min averages were recorded with a data logger (Type CR10X, Campbell Scientific Inc.,
213 Logan, UT, USA). The orchard had a tree density of 400 trees ha⁻¹ and was planted in
214 1995. In August 2002, the orchard had a leaf area index of 2.0 (measured with a plant
215 canopy analyser, model LAI-2000, LI-COR Inc., Lincoln, NE, USA) and the canopy
216 covered 45% of the ground; it maintained these characteristics during the entire
217 measurement period. The profile was obtained along the row, at one-fourth of the distance
218 between two adjacent trees of average dimension and canopy shape, inside the dripper wet
219 zone but near its edge; this position was chosen as representative of the soil volume
220 occupied by most of the root systems.

221 Daily variations of R_p with soil temperature were computed using recorded values every 10
222 min at each soil layer. For the seasonal variation analysis, in turn, noon temperatures were
223 used. In order to scale from R_p versus temperature to RR using Eq. (3), average root radius
224 data obtained from Experiment 1 were used. In addition, L_v values reported by Searles et al.
225 (2009) from an intensive olive plantation and Abrisqueta et al. (2008) for a GF677-grafted

226 peach orchard have been used to compute RR. A summary of the input values used for RR
 227 calculations is presented in Table 2.

228

229 Table 2. Input parameters for the model proposed in Eq. (4). Values for L_v have been
 230 obtained from Searles et al. (2009) for olive and from Abrisqueta et al. (2008) for the
 231 GF677 rootstock. Average root radiuses have been obtained from the scanned root systems
 232 of the plants of Experiment 1.

Soil depth (m)	Root length density, olive ($m\ m^{-3}$)	Root length density, GF677 ($m\ m^{-3}$)	Layr depth (m)	Root radius, olive (m)	Root radius, GF677 (m)
0.05	21200	14000	0.05	0.00027	0.0003
0.1	19800	4700	0.05	“	“
0.2	17200	4700	0.1	“	“
0.4	12500	14200	0.2	“	“
0.8	5540	9500	0.4	“	“

233

234 No extrapolation was applied outside the lower range of temperatures of Experiment 1 from
 235 which the functions were obtained, meaning that soil temperatures data below 10 °C were
 236 not considered. This rule has been applied because cell membrane functionality below this
 237 temperature could not be studied. In the appendix a list of abbreviations is provided.

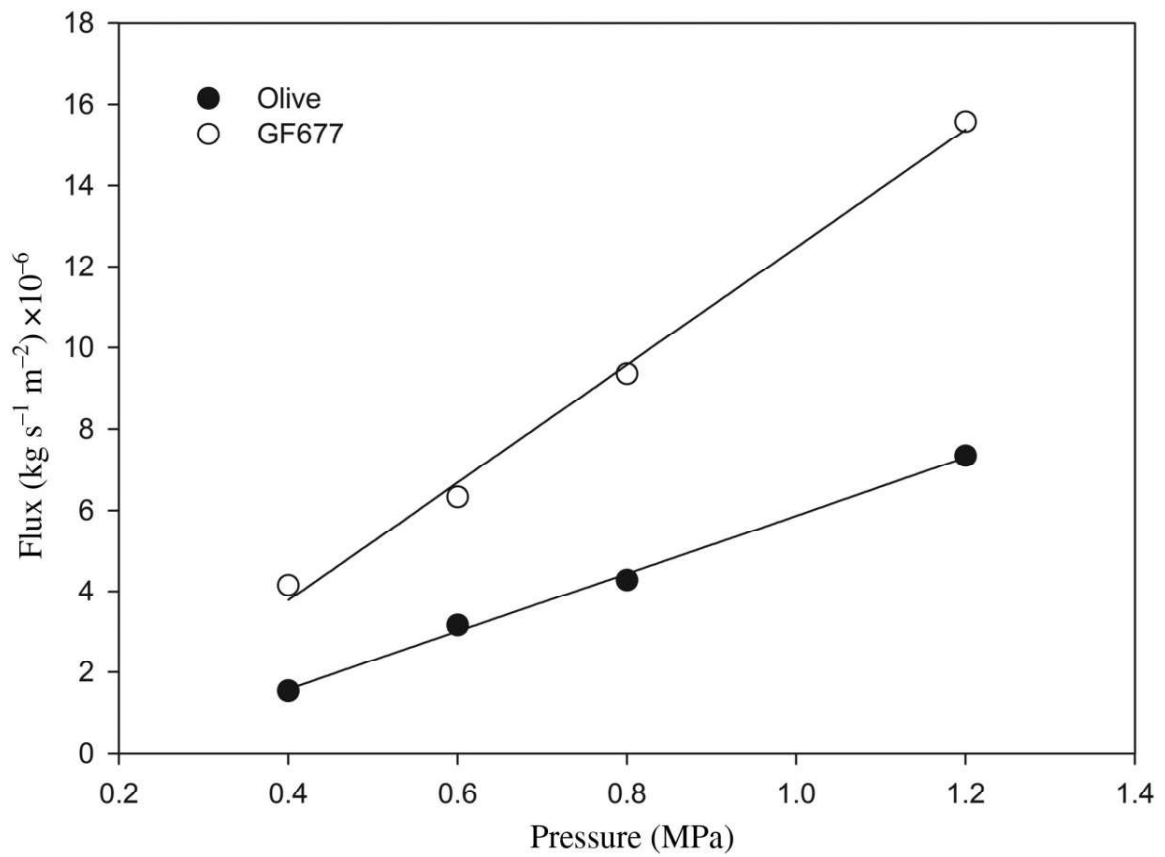
238 *Data analysis*

239 Statistical analysis of the data was performed using the program Statistic (Statistix9 for
240 Windows, Analytical Software, Tallahassee, FL, USA). An ANOVA was used to compare
241 the two almond rootstocks using the Tukey test with a level of significance of $P < 0.05$.

242 **Results**

243 *Experiment 1: effect of the temperature on radial root hydraulic specific resistance*

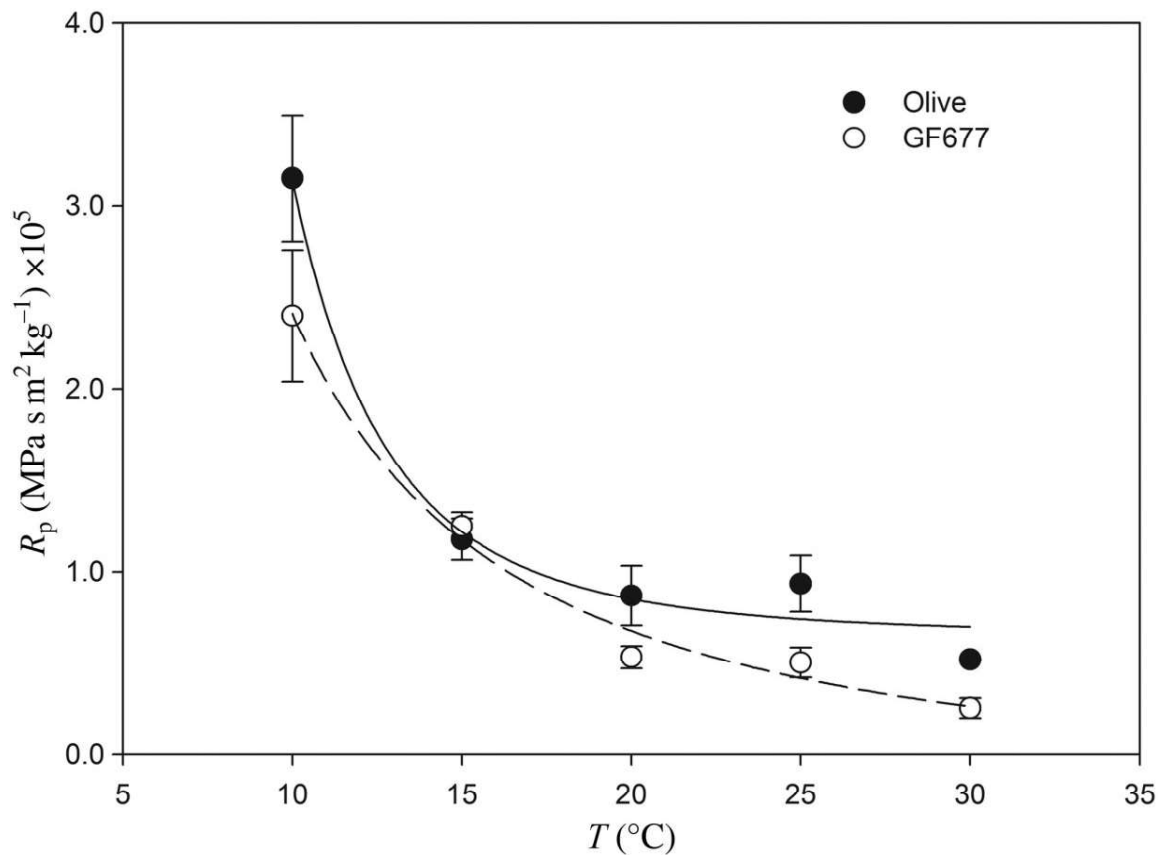
244 The pressure-flow functions showed a linear relationship at all temperatures and for all the
245 species (Figure 1); thus, a linear fit was used to compute the slope. The average R_p values
246 obtained from the inverse of the slopes at each temperature are presented in Figure 2. The
247 average values present an increase in R_p as the ambient temperature is decreased from 30 to
248 10 °C, with a 6.0-fold difference for olive and a 9.5-fold difference for GF677, between the
249 point at 30 °C and the one at 10 °C.



250

251 Figure 1. Examples of flux–pressure relations measured at 25 °C in olive and the GF677
 252 rootstock. The lines represent the linear fits. For olive: $R^2 = 0.99$, $P < 0.001$, and for
 253 GF677: $R^2 = 0.99$, $P < 0.001$.

254



255

256 Figure 2. Specific root resistance (R_p) at different temperatures for olive and GF677
 257 rootstock. Means and SDs ($n = 4$) are shown. The fitted equations for olive and GF677 are
 258 $R_p = 64934.88 + 1.09 \times 109T - 3.64$ (solid line) and $R_p = -19593.29 + 1.000 \times 107T - 1.58$
 259 (dotted line). Adjusted R^2 and significance levels are $R^2 = 0.98$, $P < 0.016$ for olive and R^2
 260 $= 0.99$, $P < 0.011$ for the GF677.

261

262 The average R_p values obtained for the GF677 rootstock were always lower than for olive
 263 trees except at 15 °C; at that point, the value of R_p of both species is nearly the same.

264 A three-parameter power function has been fitted for the two species:

265 Olive: $R_p = 64934.88 + 1.09 \times 10^9 T^{-3.64}$
266 ($R^2 = 0.98, P < 0.016$) (4)

267 GF677: $R_p = -19593.29 + 1.00 \times 10^7 T^{-1.58}$
268 ($R^2 = 0.99, P < 0.011$) (5)

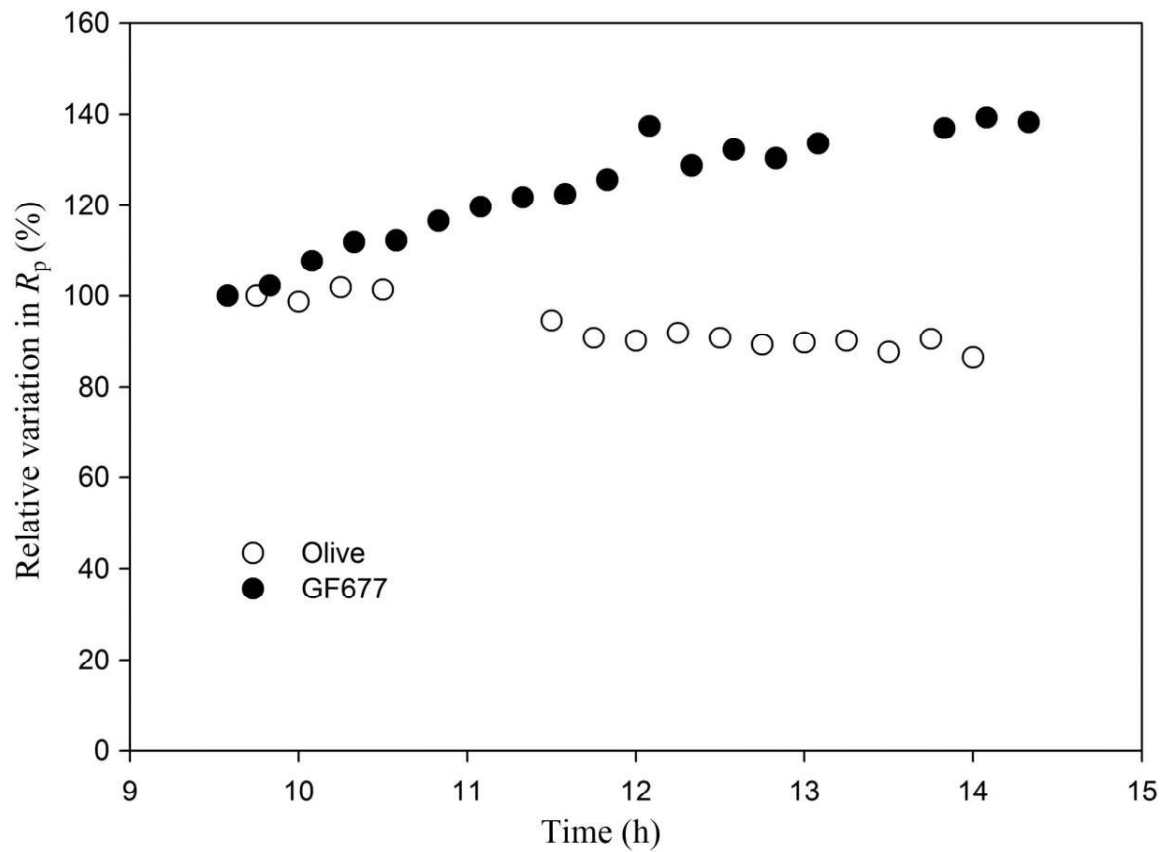
269 where R_p has the dimensions of $\text{MPa s m}^2 \text{ kg}^{-1}$.

270 *Experiment 2: comparison between rootstocks*

271 Specific resistance at 25 °C was $5.00 \times 10^4 \pm 8.22 \times 10^3 \text{ MPa s m}^2 \text{ kg}^{-1}$ for GF677 and only
272 $1.40 \times 10^4 \pm 2.81 \times 10^3 \text{ MPa s m}^2 \text{ kg}^{-1}$ for GN15; this difference was highly significant (P
273 < 0.01).

274 *Experiment 3: stability test of radial root hydraulic specific resistance in olive and GF677*

275 The resistance at a constant pressure changed over time in a different way for the two
276 studied cuttings. Olive plants maintained a quasi-steady value during the whole experiment,
277 reducing $R_p < 10\%$. In GF677, on the contrary, plants showed a larger variation, increasing
278 linearly until a maximum of 40% at the end of the experiment (Figure 3). Temperature was
279 closely monitored and recorded during both experiments; it decreased 0.9 and 0.4 °C during
280 the olive and GF677 experimental measurements, respectively.



281

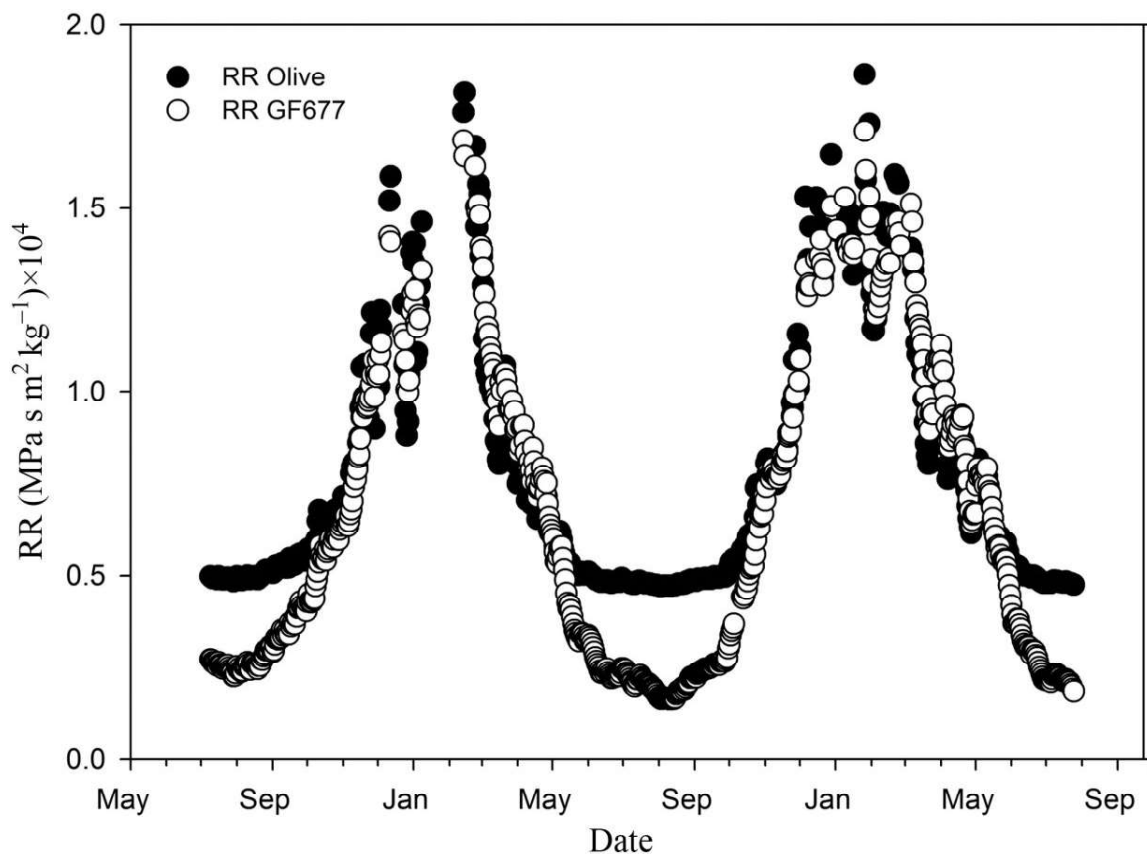
282 Figure 3. Variations in R_p at a fixed pressure (0.4 MPa) for olive (open circles) and the
 283 GF677 rootstock (filled circles) during 5 h of measurements.

284

285 *Scaling-up the radial root hydraulic specific resistance to the whole root system*

286 Equations (3)–(5) were used to compute the variations in RR of olive and GF677 due to the
 287 daily and seasonal cycles of soil temperature through two consecutive winters; the results
 288 are presented in Figures 4 and 5. Gaps during winter periods correspond to soil
 289 temperatures below the range covered by Eqs (4) and (5), i.e., 10 °C.

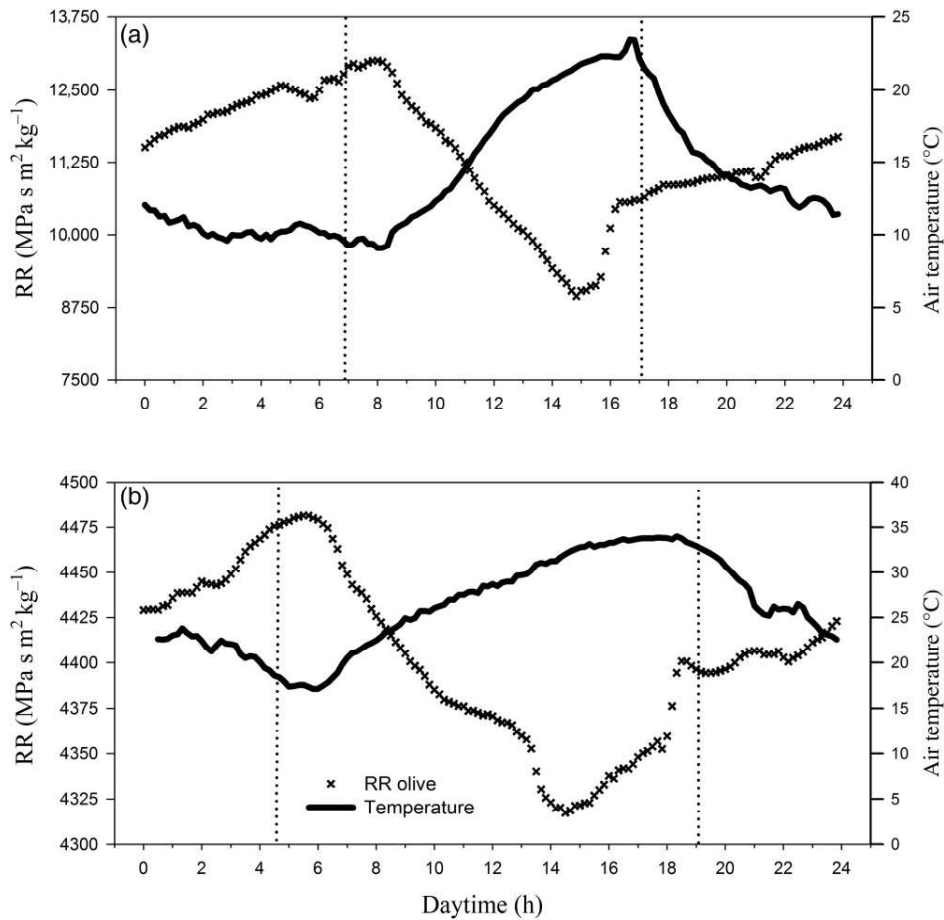
290 The computations with the model using the function for olive gave rather steady RR values
 291 $\sim 0.5 \times 10^4 \text{ MPa s m}^2 \text{ kg}^{-1}$ for the whole summer (Figure 4). Radial root system resistance
 292 increased from the first days of autumn until the end of the winter, reaching its maximum
 293 value $\sim 1.5 \times 10^4 \text{ MPa s m}^2 \text{ kg}^{-1}$ (~ 3.5 times the summer RR) in February of both years.
 294 When the winter ended, RR decreased quickly during the spring, reaching the summer
 295 value again at the beginning of June. GF677 showed a less stable root resistance during the
 296 summer period (Figure 4), changing its RR from $0.2 \times 10^4 \text{ MPa s m}^2 \text{ kg}^{-1}$ in early June to
 297 $0.15 \times 10^4 \text{ MPa s m}^2 \text{ kg}^{-1}$ in early August. Fluctuations of RR along the season followed a
 298 similar pattern as in olive, rising from the lowest values of the summer to a peak $\sim 1.46 \times$
 299 $10^4 \text{ MPa s m}^2 \text{ kg}^{-1}$ during the winter period for both years.



301 Figure 4. Calculated values of RR for olive (filled circles) and the GF677rootstock (open
302 circles). Each point represents the RR value obtained using noon temperatures at each of
303 the five soil layers for the two consecutive winters. The gaps during the winter periods
304 correspond to noncomputed values because the temperature in one or more layers was
305 below 10 °C.

306

307 Figure 5 compares two examples of the computed daily variations of RR for a winter and a
308 summer day; air temperature is also shown. Dotted lines mark the time of dawn and
309 twilight. Time of maximum and minimum values of RR appeared to be independent of the
310 season, with the maximum value occurring 1 h after dawn and the minimum value
311 occurring between 14:00 and 15:00 UTC. While the time of maximum RR was coincident
312 with the time of minimum air temperature, the minimum value of RR occurred ~2 h before
313 the time of maximum air temperature. Differences between the maximum and the minimum
314 values of RR in different seasons were related to the different amplitude of soil temperature
315 diurnal waves.



316

317 Figure 5. Daily variations of calculated RR (crosses) for olive and the corresponding air
 318 temperature (solid line) during a winter and summer day. Graph (a) corresponds to DOY 34
 319 (February) and Graph (b) corresponds to DOY 184 (June). Dotted lines represent dawn and
 320 twilight hours.

321

322 Discussion

323 The results of Experiment 1 show that an increase in R_p —both for olive and the GF677
 324 rootstock—occurs when the root system is exposed to low temperatures. Our calculations
 325 suggest that this effect would have an implication for modelling transpiration in periods

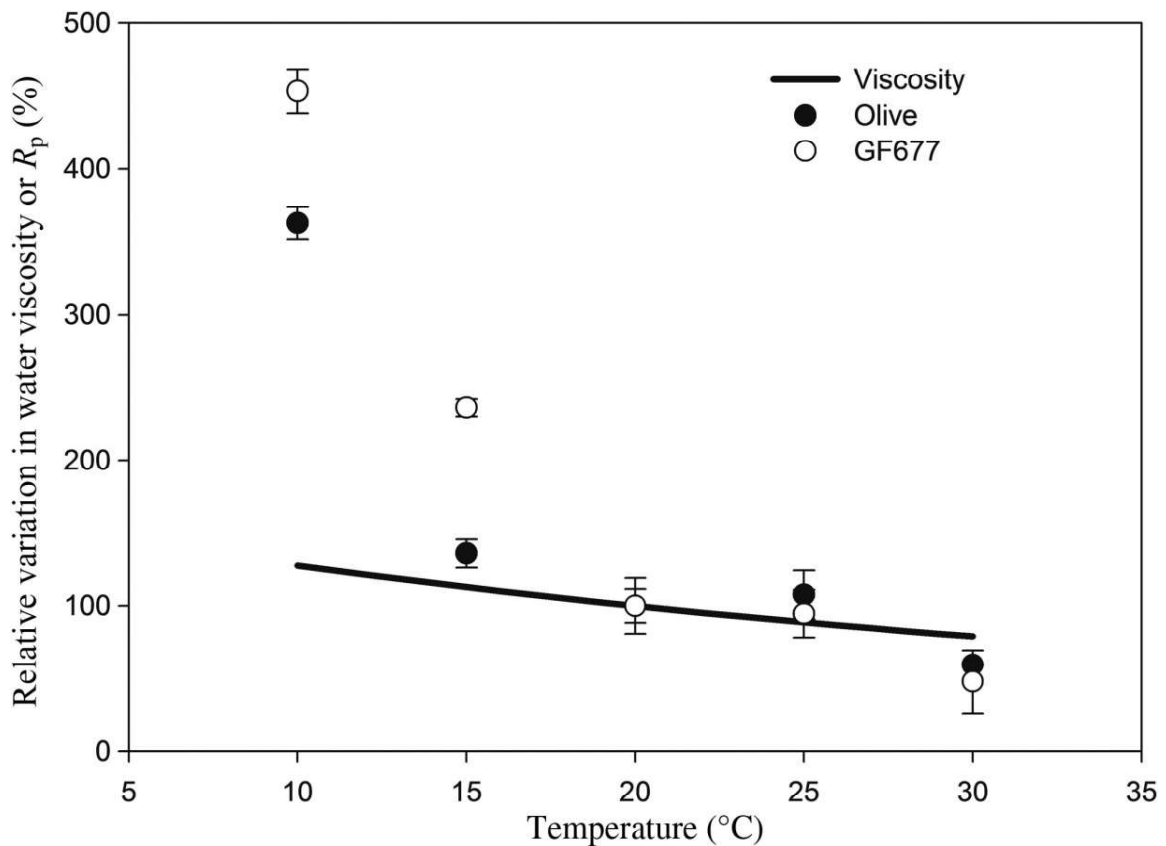
326 when soil temperature is relatively low (Figures 2, 4 and 5). Differences in the water uptake
327 ability of the roots between cultivars has also been exposed in Experiment 2, showing that
328 significant differences in the absolute values of R_p can be expected within the same species.

329 *Variations of plant resistance*

330 Values of R_p reported in the literature for other species refer to a single temperature, usually
331 20 °C. At that temperature, large interspecific differences can be found, ranging from $3 \times$
332 10^7 MPa s m² kg⁻¹ for maize (*Zea mays* L), 1×10^{10} MPa s m² kg⁻¹ for *P. tremuloides* or 1
333 $\times 10^5$ MPa s m² kg⁻¹ for sunflower (*Helianthus annuus* L) (Frensch and Steudle 1989,
334 Ameglio et al. 1990, Wan et al. 2001). In his work with sunflower, Ameglio et al. (1990),
335 reported an increase of one order of magnitude at 4 °C with regard to its value at 20 °C;
336 Running and Reid (1980) in *Pinus contorta* Douglas and Norisada et al. (2005) in
337 *Cryptomeria japonica* D.Don accounted for relative variations of 4.4- and 2.2-fold for a
338 temperature range of 20–0 °C in the first case and 30–5 °C in the second. The relative
339 change of R_p with temperature found in olive and GF677 is shown in Figure 6. The results
340 are closer to those found in sunflower by Ameglio et al. (1990) than for the other species in
341 the literature.

342 The underlying mechanism for the observed changes in R_p has been a matter of controversy
343 since the first experiments developed by Kramer (1940) with tomato plants. In his work,
344 variations in water viscosity were suggested as the main factor producing the increases in
345 R_p and the observed reductions in transpiration. Later studies have shown that under low
346 temperatures (below 15 °C), increases in R_p do not follow the expected changes in water
347 viscosity, and modifications in cell membrane structure and/or aquaporin number and

348 activity have been hinted as the responsible cause (Kaufmann 1975, 1977, Grossnickle
349 1988, Wan et al. 2001). Kuiper (1964) first proposed that combinations of both factors—
350 water viscosity and modifications in the membrane structure—are involved in the
351 phenomenon. The author pointed out that a critical threshold value exists, and the
352 temperatures below that limit trigger changes in membrane structure, increasing R_p to a
353 greater extent than that expected by the increase in water viscosity. Our results fully
354 support Kuiper's hypothesis: Figure 6 represents our measurements of the relative changes
355 to R_p together with the relative variations in water viscosity, calculated following Roderick
356 and Berry (2001). The change in water viscosity does not explain the observed changes in
357 R_p when the temperature is lower than 15 °C, a threshold that seems common to both
358 cultivars analysed (Figure 6). Wan et al. (2001) came to the same conclusion with *P.*
359 *tremuloides*, finding a relative variation in R_p of 3.5 times when changing root temperature
360 from 20 to 5 °C, while water viscosity only varied 1.5 times for the same temperature
361 range. Figure 6 also shows that the deviation from the viscosity is not only produced at low
362 temperatures; both olive and GF677 exhibit lower values of R_p than that expected due to
363 viscosity changes at 30 °C. This is in accordance with the observations made by Cochard et
364 al. (2000) for *Quercus robur* L.



366

367 Figure 6. Relative variation in viscosity and R_p for olive (filled circles) and the GF677
 368 rootstock (open circles) with regard to its value at 20 °C. The line represents the computed
 369 variation of the viscosity with the temperature using the equation proposed by Roderick and
 370 Berry (2001). The circles are the means and the bars represents the SD ($n = 4$).

371

372 Although these important variations of R_p with temperature have been described for various
 373 species, the practical implications of a temperature-dependent R_p in modelling E_p are
 374 unknown. Figures 4 and 5 represent an attempt of quantifying total root resistance changes
 375 as a function of soil temperature in a real orchard. The seasonal thermal regime of a given

376 soil is determined by the climate, the degree of shading and the soil hydrological and
377 physical characteristics. In this sense, the experimental site used to collect soil temperature
378 profile data is reasonably representative of an irrigated, intensive tree orchard in southern
379 Spain on a medium texture soil, with minor or null regard to what the cultivated species
380 actually is.

381 Values of RR presented in Figure 4 exhibit variations between summer and winter ~ 3.5
382 times for olive and 9 times for GF677. Experiments have revealed that a reduction of
383 stomatal conductance occurs due to changes in the soil temperature environment
384 (Kaufmann 1982, Wan et al. 2001, Apostol et al. 2007). The observed reduction in stomatal
385 conductance has been explained by the larger increase of RR in relation to R_{plant} when the
386 root environment is chilled (Running and Reid 1980, Pavel and Fereres 1998). In fact, for
387 olives in the field, water-stress-like behaviour under wet soil conditions (when R_s is
388 negligible compared with R_p) is frequent under Mediterranean climates, where rain is
389 concentrated during winter and spring. This phenomenon has been demonstrated to be
390 related to an increase in RR of the tree (López-Bernal et al. 2015).

391 The RR increases during winter in GF677 are of course less relevant on a practical basis, as
392 GF677 is always grafted with deciduous scions, the leafless period of which varies with the
393 climate of the area and with the species/cultivar of the scion. Nevertheless, when
394 transpiring leaves are present during spring and autumn, a significant variation in RR may
395 still be expected, as can be observed in Figure 4. Apostol et al. (2007) demonstrated that the
396 lower soil temperatures during spring in the deciduous tree *Q. rubra* significantly reduce E_p
397 and stomatal conductance early shooting fruit scions may well experience significantly
398 higher RR than in summer with an already considerable leaf area. For example, an almond

399 scion grafted on GF677 would have to deal with $RR \sim 0.64 \times 10^4 \text{ MPa s m}^2 \text{ kg}^{-1}$ at the end
400 of April (Figure 4), meaning 3.5-fold the RR of July with a leaf area only 30% less than
401 that of full summer (E. Fereres, personal communication).

402 It must be considered that in the simulation of Figure 4, a fixed value of L_v has been applied
403 for the entire simulation period, meaning that RR could be overestimated for the intervals
404 where new root production occurs. Fernández et al. (1992) observed for olive cv.
405 ‘Manzanillo’ under different irrigation regimes that root production is concentrated in late
406 spring and in early autumn for rainfed trees, while for irrigated trees, root production occurs
407 from spring to autumn. In a more general study on temperate tree species, McCormack et
408 al. (2014) discovered that most new root production is concentrated during late spring (and
409 also during late summer), periods where RR in the simulation (Figure 4) is at its minimum.
410 Hence, including L_v changes in the model simulation would likely increase the difference
411 between the seasons.

412 Giving attention to the summer period, a remarkable difference in the trend of RR can be
413 observed in Figure 4 for both cultivars. While a reduction of sixfold in RR from May to
414 August appears in the GF677 rootstock, RR remains almost constant for olive at the same
415 period. This behavioural difference can be explained by the different sensibility of R_p to
416 higher temperatures (over 20 °C) of both cultivars presented in Figure 2. It would be
417 expected that under the same soil water content and atmospheric demand, GF677 would
418 have a more favourable water status than olive since a lower RR would lead to a higher Ψ_l .
419 Although it is difficult to discuss the theoretical outcomes on E_p of a variable RR without
420 accounting for the other components of the resistance catena with the aid of a full SPAC

421 model, it is self-evident from Figure 4 that without a specifically calibrated function of R_p
422 versus temperature, the accuracy of such a model would be dramatically reduced.

423 Accounting for the seasonal variation in RR like in Figure 4 is subjected to the availability
424 of soil temperature profile records, which are rarely available. Jackson et al. (1996) proved
425 that almost 50% of the roots of a tree are typically concentrated in the first 25 cm of soil.
426 With those numbers in mind, one might consider using mean air temperature as a surrogate
427 for soil temperature, but what error should we expect from such an assumption? In the daily
428 patterns of olive RR represented in Figure 5 (GF677 data are not shown for clarity, but it
429 behaves similarly), it is noteworthy that maximum and minimum values of RR occur,
430 respectively, ~ 1 h after dawn and between 14:00 and 15:00 UTC, independently of the
431 season. Figure 5 indicates that maximum RR is coincident with minimum air temperature,
432 whereas minimum RR is not in phase with the time of maximum air temperature. In fact,
433 when air temperature is approaching its maximum value, between 14:00 and 18:00 UTC,
434 RR has already inverted its trend and is again increasing instead of decreasing, as expected
435 according to Eq. (4) (see Figure 2). This result might be associated with the fact that tree
436 crown is intercepting part of the incoming radiation, reducing the amount of energy
437 reaching the soil surface. Despite this phase mismatch, daily mean air temperature may still
438 be valid as a substitute of soil temperature in order to capture the seasonal changes shown
439 in Figure 4. Table 3 depicts average monthly root mean square values (RMSE) between RR
440 computed using average daytime (between dawn and twilight) air temperature and mean
441 RR using soil temperature records. For olive, the error is expected to range between 20%
442 during winter and $< 2\%$ in summer, while for GF677, the error is relatively constant and
443 would be $\sim 20\%$ across all seasons. Thus, the convenience of using mean air temperature

444 instead of soil temperature depends on the species simulated, and should be evaluated on
445 the basis of the required precision in the estimation of mean RR. When RR is critical for
446 modelling tree E_p and no soil temperature is available, the use of a soil temperature model
447 may be preferable to the direct use of air temperature.

448

449 Table 3. Average monthly RMSE from RR values computed using mean daytime air
450 temperature and mean RR calculated using soil temperature records for olive and GF677.

Month	RMSE (MPa s m ² kg ⁻¹)	
	Olive	GF677
January	4204.9	2790.5
February	3940.1	2296.7
March	2821.9	2589.1
April	1003.3	1159.5
May	461.2	730.7
June	104.3	331.3
July	84.5	304.2
August	70.9	270.1
September	121.4	315.9
October	744.6	892.2
November	1462.5	1181.2
December	3357.3	2069.2

451

452 *Uncertainties in the measurement of radial root hydraulic specific resistance*

453 Cyclic variations in R_p have been described for different plant species, and variations in
454 aquaporin expression have been proposed as a possible cause of the daily changes in root
455 hydraulic specific resistance (Henzler et al. 1999, Tsuda and Tyree 2000, Tyree and
456 Zimmermann 2002, Caldeira et al. 2014). The results of Experiment 3 (Figure 3) present a
457 change in R_p during the measurement period and show two different patterns for the two
458 studied cultivars that could not be attributed to temperature variations, since they changed
459 less than one degree inside the growth chamber through the whole experiment.

460 From figure 3, one may think that the variation present in the GF677 rootstock may be due
461 to a circadian rhythm in R_p , however, the magnitude of such change is of lower degree than
462 those observed by Henzler et al. (1999) for *L. japonicus* and by Tyree and Zimmermann
463 (2002) for tobacco plants. Besides, Caldeira et al. (2014) demonstrated, when studying
464 maize plants, that non-circadian variations appear at low evaporative demand, a common
465 condition when using growth chambers. This information led us to think that the observed
466 increase in R_p for GF677 may well be an artefact related to the methodology applied.
467 Espino and Schenk (2011) demonstrated that even under positive pressure, xylem cavitation
468 can occur, resulting in an increase of measured R_p . The same authors proposed the lateral
469 flow out from xylem vessels as another cause inducing an artificial increase in R_p (Espino
470 and Schenk 2011). The fact that only the GF677 rootstock presents an increase on R_p and
471 the olive did not could be attributed to anatomical differences between them, although we
472 have no proof of this.

473 Regardless of the mechanisms implied, the increase in R_p in steady conditions of
474 temperature and pressure that we observed in GF677 did not have an impact on the
475 determination of R_p values obtained when changing the applied pressure. Evidence of it is
476 the linearity of the relationship between pressure and flux (Figure 1). The linear functions
477 fitted to the measurements, to compute R_p at the different temperatures, all have a $R^2 \sim 0.90$
478 (data not shown). If the variation observed in Figure 3 has had an impact on the
479 measurements, a curvilinear response should have been observed in the flux–pressure
480 relationships like that of Figure 1.

481 *Radial root hydraulic specific resistance differences between rootstocks*

482 The result of Experiment 2 exhibits a highly significant difference between the two
483 rootstocks studied. The experiment was performed at one temperature only and with a
484 reduced number of plants; hence, further research is needed in order to clarify whether the
485 difference we found is also present at other temperatures. If this difference has a genetic
486 origin, measuring R_p could be an interesting trait to evaluate the performance related to
487 water use for a variety of rootstocks under specific environments, since R_p is directly
488 related to the water uptake capacity of a root, and can be easily incorporated into SPAC
489 models.

490 According to our results, root hydraulic resistance can no longer be considered a steady
491 feature of the hydraulic pathway; the transpiration rate, the water uptake and the plant water
492 status do not depend only on canopy demand and water availability but may be heavily
493 influenced by soil temperature. Hence, it would be advisable to include R_p variation

494 functions with temperature in SPAC models in order to properly estimate E_p , considering
495 that of all the resistances composing the plant system analogy, R_p is usually the highest one.

496

497 **Funding**

498 This work was supported by project AGL-2010-20766 of the Spanish Ministry of Economy
499 and Competitiveness (former Ministry of Science and Innovation) and by the European
500 Community's Seven Framework Programme-FP7 (KBBE.2013.1.4- 09) under grant
501 agreement no. 613817 (MODEXTREME, modextreme.org).

502 **Acknowledgments**

503 We thank both the 'FPI' programme of the aforementioned ministry and the JAE
504 programme of the Spanish Research Council (CSIC) for providing the Ph.D. scholarships
505 granted to the O.G.-T. and F.O., respectively. We also thank Manolo Gonzalez, Maria
506 Roman, Jose Luis Vazquez, Marcos Orgaz and Rafaela Gutierrez for the excellent technical
507 assistance provided.

508 **Conflict of interest**

509 None declared.

510 **Appendix**

511 Abbreviation list

Symbol	Description	Units
--------	-------------	-------

a	Root radius	(m)
d	Depth of the soil layer	(m)
E_p	Transpiration rate	($\text{kg m}^{-2} \text{s}^{-1}$)
L_v	Root length density	(m m^{-3})
RR	Resistance of the total root system per square meter of soil in the radial direction	($\text{MPa s m}^{-2} \text{kg}^{-1}$)
R_{soil}	Resistance from the soil to the root xylem	($\text{MPa s m}^{-2} \text{kg}^{-1}$)
R_{plant}	Resistance from root xylem to leaves	($\text{MPa s m}^{-2} \text{kg}^{-1}$)
R_s	Radial root hydraulic specific resistance from the soil to the root surface	($\text{MPa s m}^{-2} \text{kg}^{-1}$)
R_p	Radial root hydraulic specific resistance per square meter of root from the root surface	($\text{MPa s m}^{-2} \text{kg}^{-1}$)
Ψ_1	Leaf water potential	(MPa)
Ψ_{mid}	Midday water potential	(MPa)
Ψ_{soil}	Soil water potential	(MPa)

512

513 **References**

514 Abrisqueta JM, Mounzer O, Álvarez S, Conejero W, García-Orellana Y, Tapia LM, Vera J,
515 Abrisqueta I, Ruiz-Sánchez MC (2008) Root dynamics of peach trees submitted to partial
516 rootzone drying and continuous deficit irrigation. *Agric Water Manage* 95:959–967.

517 Ameglio T, Morizet J, Cruiziat P, Martignac M, Bodet C, Raynaud H (1990) The effects of
518 root temperature on water flux, potential and root resistance in sunflower. *Agronomie*
519 10:331–340.

520 Apostol KG, Jacobs DF, Wilson BC, Salifu KF, Dumroese RK (2007) Growth, gas
521 exchange, and root respiration of *Quercus rubra* seedlings exposed to low root zone
522 temperatures in solution culture. *For Ecol Manag* 253:89–96.

523 Axelsson B, Ågren G (1976) *Tree growth model (PT 1)—a development paper*. Swedish
524 Coniferous Forest Project Internal Report 41.

525 Caldeira CF, Jeanguenin L, Chaumont F, Tardieu F (2014) Circadian rhythms of hydraulic
526 conductance and growth are enhanced by drought and improve plant performance. *Nat*
527 *Commun* 5:5365. doi:10.1038/ncomms6365

528 Campbell GS (1985) Transpirations and plant water relations. In: Campbell GS (ed) *Soil*
529 *physics with basic: transport models for soil–plant systems*. Elsevier Science B.V.,
530 Amsterdam, pp 122–133.

531 Cochard H, Martin R, Gross P, Bogeat-Triboulot MB (2000) Temperature effects on
532 hydraulic conductance and water relations of *Quercus robur* L. *J Exp Bot* 51:1255–1259.

533 Couvreur V, Vanderborcht J, Javaux M (2012) A simple three-dimensional macroscopic
534 root water uptake model based on the hydraulic architecture approach. *Hydrol Earth Syst*
535 *Sci* 16:2957–2971.

536 Doussan C, Vercambre G, Pagè L (1998) Modelling of the hydraulic architecture of root
537 systems: an integrated approach to water absorption—distribution of axial and radial
538 conductances in maize. *Ann Bot* 81:225–232.

539 Espino S, Schenk HJ (2011) Mind the bubbles: achieving stable measurements of
540 maximum hydraulic conductivity through woody plant samples. *J Exp Bot* 62:1119–1132.

541 Fernández JE, Moreno F, Martín-Aranda J, Fereres E (1992) Olive-tree root dynamic under
542 different soil water regimes. *Agric Med* 122:225–235.

543 Frensch J, Steudle E (1989) Axial and radial hydraulic resistance to roots of maize (*Zea*
544 *mays* L.). *Plant Physiol* 91:719–726.

545 Grossnickle SC (1988) Planting stress in newly planted jack pine and white spruce. 1.
546 Factors influencing water uptake. *Tree Physiol* 4:71–83.

547 Henzler T, Waterhouse RN, Smyth AJ, Carvajal M, Cooke DT, Schäffner AR, Steudle E,
548 Clarkson DT (1999) Diurnal variations in hydraulic conductivity and root pressure can be
549 correlated with the expression of putative aquaporins in the roots of *Lotus japonicus*. *Planta*
550 210:50–60.

551 Hertel A, Steudle E (1997) The function of water channels in *Chara*: the temperature
552 dependence of water and solute flows provides evidence for composite membrane transport
553 and for a slippage of small organic solutes across water channels. *Planta* 202:324–335.

554 Jackson RB, Canadell J, Ehleringer JR, Mooney HA, Sala OE, Schulze ED (1996) A global
555 analysis of root distributions for terrestrial biomes. *Oecologia* 108:389–411.

556 Kaufmann MR (1975) Leaf water stress in Engelmann spruce: influence of the root and
557 shoot environments. *Plant Physiol* 56:841–844.

558 Kaufmann MR (1977) Soil temperature and drying cycle effects on water relations of *Pinus*
559 *radiata*. *Can J Bot* 55:2413–2418.

560 Kaufmann MR (1982) Evaluation of season, temperature, and water stress effects on
561 stomata using a leaf conductance model. *Plant Physiol* 69:1023–1026.

562 Kramer PJ (1940) Root resistance as a cause of decreased water absorption by plants at low
563 temperatures. *Plant Physiol* 15:63–79.

564 Kuiper PJC (1964) Water uptake of higher plants as affected by root temperature. *Meded*
565 *Landbouwhogeschool Wageningen* 64:1–11.

566 Lee SH, Singh AP, Chung GC, Ahn SJ, Noh EK, Steudle E (2004) Exposure of roots of
567 cucumber (*Cucumis sativus*) to low temperature severely reduces root pressure, hydraulic
568 conductivity and active transport of nutrients. *Physiol Plant* 120:413–420.

569 López-Bernal Á, García-Tejera O, Testi L, Orgaz F, Villalobos FJ (2015) Low winter
570 temperatures induce a disturbance of water relations in field olive trees. *Trees* 29:1247–
571 1257.

572 McCormack ML, Adams TS, Smithwick EAH, Eissenstat DM (2014) Variability in root
573 production, phenology, and turnover rate among 12 temperate tree species. *Ecology*
574 95:2224–2235.

575 Mellander PE, Stähli M, Gustafsson D, Bishop K (2006) Modelling the effect of low soil
576 temperatures on transpiration by Scots pine. *Hydrol Process* 20:1929–1944.

577 Norisada M, Hara M, Yagi H, Tange T (2005) Root temperature drives winter acclimation
578 of shoot water relations in *Cryptomeria japonica* seedlings. *Tree Physiol* 25:1447–1455.

579 Pavel EW, Fereres E (1998) Low soil temperatures induce water deficits in olive (*Olea*
580 *europaea*) trees. *Physiol Plant* 104:525–532.

581 Roderick ML, Berry SL (2001) Linking wood density with tree growth and environment: a
582 theoretical analysis based on the motion of water. *New Phytol* 149:473–485.

583 Running SW, Reid CP (1980) Soil temperature influences on root resistance of *Pinus*
584 *contorta* seedlings. *Plant Physiol* 65:635–640.

585 Sachs J (1870) Movement of water in plants. In: Sachs J (ed) Textbook of botany
586 morphological and physiological book III. Cambridge University press, pp 598–614.

587 Searles PS, Saravia DA, Rousseaux MC (2009) Root length density and soil water
588 distribution in drip-irrigated olive orchards in Argentina under arid conditions. *Crop*
589 *Pasture Sci* 60:280–288.

590 Tsuda M, Tyree MT (2000) Plant hydraulic conductance measured by the high pressure
591 flow meter in crop plants. *J Exp Bot* 51:823–828.

592 Tyree M, Zimmermann MH (2002) Variable hydraulic conductance: temperature, salts and
593 direct plant control. In: Tyree M, Zimmermann MH (eds) Xylem structure and the ascent of
594 sap. Springer, Heidelberg, pp 205–214.

- 595 Van den Honert TH (1948) Water transport in plants as a catenary process. Discuss Faraday
596 Soc 3:146–153.
- 597 Wan X, Zwiazek JJ, Lieffers VJ, Landhäusser SM (2001) Hydraulic conductance in aspen
598 (*Populus tremuloides*) seedlings exposed to low root temperatures. Tree Physiol 21:691–
599 696.
- 600 Williams M, Law BE, Anthoni PM, Unsworth MH (2001) Use of a simulation model and
601 ecosystem flux data to examine carbon-water interactions in ponderosa pine. Tree Physiol
602 21:287–298.
- 603 Yamamoto R (1995) Dependence of water conductivity on pressure and temperature in
604 plant stems. Biorheology 32:421–430.